REASSESSMENT OF THE INTENSITY OF STRONG MOTIONS EXPERIENCED DURING THE VARTHOLOMIO (W.GREECE) 1988 EARTHQUAKE

G-Akis TSELENTIS*, Jiana VASILIOU**, Efthimios SOKOS*, Panos TSARPALIS* and Dimitris RUBAS*

Abstract : A synthesis of ground motion at the damaged city of Vartholomio during the 1988 M_S=5.9 earthquake is made by means of numerical analysis employing two-dimensional modelling. The expected strong motions at the bedrock were synthesised taking into consideration the recorded motions at the nearby city of Amaliada. The thickness of the overlaying soft formations and the topography of the seismic bedrock was assessed by employing high resolution seismic reflection profiles, while the dynamic properties of the encountered formations were estimated from the dispersive characteristics of artificially generated surface waves. The seismic response analysis of the region justified the pattern of damage distribution of buildings and the characteristic macroseismic observations seem to be explained by the combined effect of the presence of low velocity surface layers and the topography of the seismic bedrock.

1 Introduction

Site conditions play a major role in establishing the damage potential of incoming seismic waves from major earthquakes. In Greece, there have been recently many consistent macroseismic observations showing that seismic structural damages may be attributed to the soft soil effects on seismic amplification and shift of the predominant period to the unfavourable range (e.g. Tselentis et al 1992, Tselentis et al 1994, Pitilakis et al 1992).

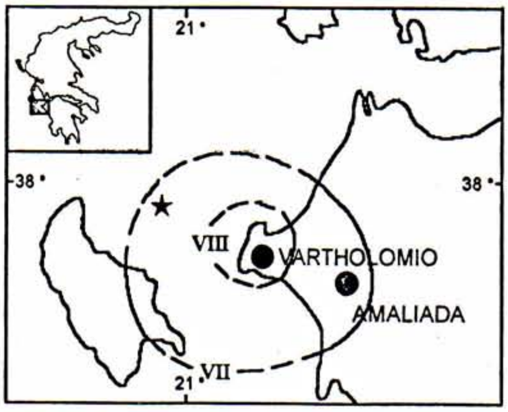

Fig.1 : Generalised isoseismal map of the October 16, 1988 M_S=5.9 earthquake.

* University of Patras, Seismological Laboratory, Rio 261 10, Greece.
** Public Works Research Laboratory, 166 Pireu Str., Athens 118 54, Greece.

On October 16, 1988 a shallow earthquake of magnitude M_S=5.9 occurred in the area of central Ionian sea (Fig.1). Macroseismic observations in NW Pelloponnesse revealed that (MM) seismic intensities reached up to VIII, at the city of Vartholomio, a value which has been higher than normally expected from that particular magnitude at that epicentral distance. Also great consistent differences in structural damage characterised the city of Vartholomio, which is the subject of the present investigation.

2 Geological regime

The city of Vartholomio and surroundings is characterised by intense neotectonic deformation and high seismicity. More specifically, this area is part of the neotectonic depression (graben) of Pirgos, which is a first order neotectonic structure.

The Alpine formations that outcrop to the east and the west of Vartholomio correspond to Gavrovo and Ionian isopic zones respectively. They gradually submerge and create an elongated tectonic depression striking N-S. At the city of Vartholomio and surroundings, the following three categories of geological formations can be located, in geochronological order (Lekkas et al 1992):

-The Vounargo formation comprising of a large variety of sandstones and shales, having a total thickness of more than 500m. This formation outcrops to the west of Vartholomio and underlies the following two lithological units:

-Calcitic sandstones which locally contain fine or coarser material from various rocks. This unit has a thickness of up to 20m and develops unconformably over the Vounargo formation. It outcrops both west of Vartholomio and at some location within the city.

-Alluvial formations which develop unconformably over the previous formation and occupy the major plain of Vartholomio. They consist of clayey sands and sandy clays with an increasing thickness towards the east.

3 Damage pattern

The behaviour of buildings during earthquakes depends upon a great number of parameters. In the city of Vartholomio which is a typical Greek city, there are buildings of different types, ages, number of stories and material properties, usually supported laterally by other buildings and showing discontinuities in height and plan.

Vartholomio's building stock is composed mainly of modern middle size buildings and a considerable number of old buildings. The spatial distribution of both types of buildings can be considered rather homogeneous.

In order to quantify the earthquake effects on the city's building stock and reveal any site specific dependence, we constructed a preliminary Geographic Information System (GIS) database by digitizing existing planning maps provided to us by the Municipality (Fig.2b). On the same database we included information describing the encountered damages which were graded into three main categories: small, significant but repairable and non-repairable.

From the 1153 buildings examined, the 173 experienced severe structural damage and had to be demolished, while 770 buildings suffered major structural damage and had to be repaired before reoccupation.

A first order assessment of the density of damages along a W-E line crossing the city was calculated using data from GIS. Judging from this figure we can see an eastwards linear increase of the density of damages. This feature was first noticed by Lekkas (1992) and was attributed to the effects of the underlying geology (Fig.2a).

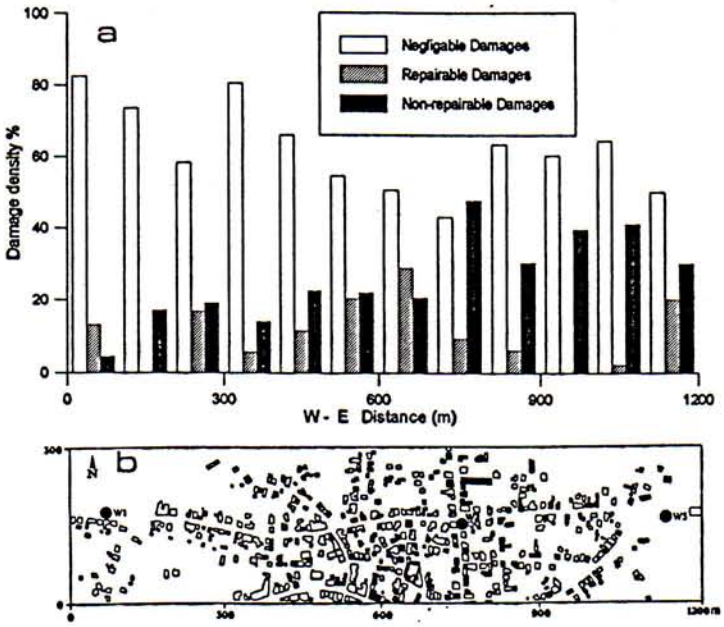

Fig.2 : a) The distribution of damage density along a W-E line crossing the city. b) A simplified map of the city. The demolished buildings are filled, the sites of the three boreholes are also shown (black circles).

4 Geophysical investigations

A geophysical survey was planed in order to understand the spatial distribution of the underlying geological formations. In total we conducted 5 Schlumberger geoelectric soundings, 5 overlapping refraction lines and 3 shallow reflection profiles with a geophone spacing of 10m (Fig.3).

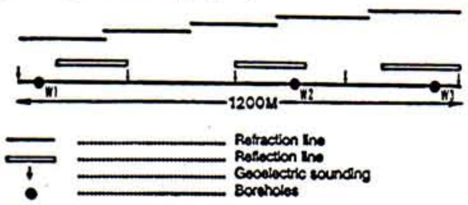

Fig.3 : Geophysical investigations carried out along a W-E section crossing the city.

The seismic instrument used was an ABEM Terraloc Mark3, 24 channel seismograph and seismic waves were generated employing a Buffalo gun. The processing of the refraction line was performed by employing ray tracing inverse modelling, using the program GLI3D (Hampson and Russell 1993), while the processing of the reflection survey was performed using PROMAX. The combined interpretation of the collected geophysical data resulted in the following simplified velocity model along a W-E section crossing the city (Fig.4).

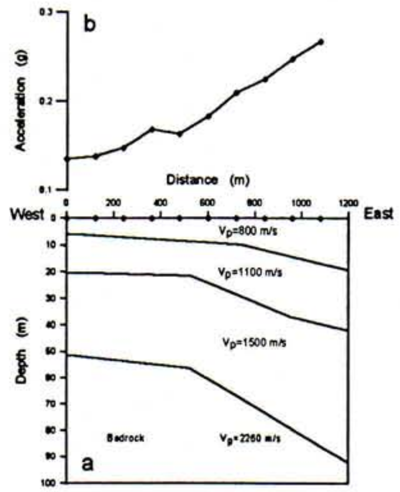

Fig 4 : a) Simplified velocity model of the investigated area, the locations of calculated synthetic seismograms are also shown (black circles). b) Peak value accelerations for the ten sites along a W-E line crossing the city.

5 Geotechnical investigations

Three boreholes were drilled (W1,W2,W3) at depths of 51.8m, 154m and 75.6m respectively (Fig.2b). At all the boreholes we carried out insitu standard penetration tests (S.P.T) at 1.5m intervals. The soil samples were subjected to classification tests and undisturbed sample tests were also carried out for the determination of the wet bulk density γ.

Furthermore, cross-hole tests were also performed. The S.P.T. mechanism, rich in shear wave energy was used as a mechanical impulse source. Fig.5 depicts the obtained shear wave velocity and S.P.T. profiles at the three sites.

The geotechnical properties of the formations lying between the three exploratory boreholes were assessed by employing surface wave dispersion techniques. By dropping a 0.5 tone weight, Rayleigh waves were generated and were recorded on 12 channels. Next the corresponding dispersion curve was evaluated and was inverted by employing the methodology proposed by Tselentis and Delis (1991), resulting in the depth variation of shear modulus and shear wave velocity.

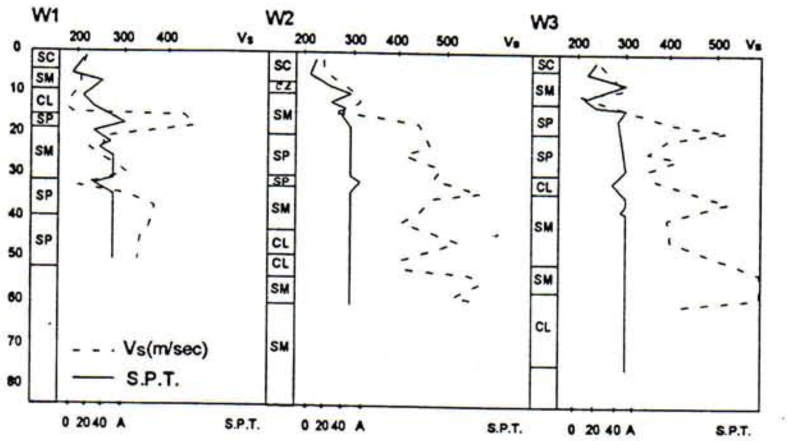

Fig.5 : Results from geotechnical investigations.

6 Evaluation of base motions

At Vartholomio, the city which experienced the heaviest damages during the event, ground acceleration was not recorded. On the other hand, records of ground acceleration were obtained at a distance of about 20km to the SE at the nearby city of Amaliada (Fig.6). We used these recordings to synthesise the base motion at Vartholomio in the following way:

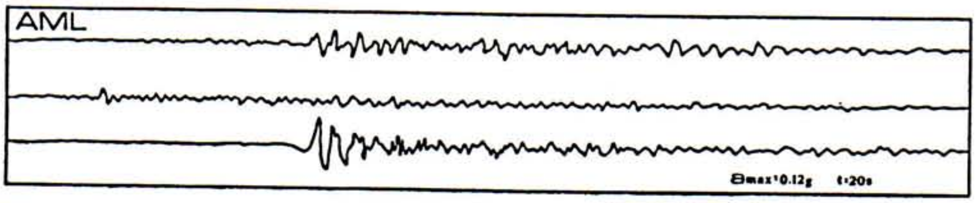

Fig.6 : Strong motion records obtained at Amaliada station.

First, the input motions at the seismic basement of the recording site at Amaliada were assessed employing SHAKE91 (Idriss and Sun 1992) deconvolution, taking into consideration the geotechnical properties of the upper formations. Next, the motion at the seismic basement of Vartholomio was analytically synthesised according to the formula:

$$a(t) = \frac{1}{2\pi}\int A_r(\omega)e^{-\frac{\pi f \Delta R}{QV_s}} e^{i\omega t} d\omega \qquad (1)$$

where $A_r(\omega)$ is the Fourier spectrum of the deconvolved record at Amaliada station, ΔR the difference in epicentral distance between the two sites, Vs the shear wave velocity at the basement and Q the quality factor. Assuming a representative range of values for the region of Q between 50 and 100 (Tselentis 1993), the corresponding base motions at Vartholomio were assessed. From these, we selected as the most representative for the site, the one which resulted in a peak value which was in agreement with the attenuation law proposed by Theodulidis and Papazachos (1992), corresponding to a value of Q=70 and depicting a peak acceleration of 0.17g.

7 Evaluation of surface motions

In order to evaluate the wave field at the surface, we employed a 2D finite difference method (FD) for solving the SH-wave equation in the heterogeneous medium depicted by the model in Fig.4. The following basic equation of motion for SH waves was used

$$\frac{\partial}{\partial x}(\mu \frac{\partial u}{\partial x}) + \frac{\partial}{\partial z}(\mu \frac{\partial u}{\partial z}) = \rho \frac{\partial^2 u}{\partial t^2} \qquad (2)$$

where u(x,z) is the displacement, $\rho(x,z)$ the density, t the time and $\mu(x,z)$ the shear modulus. The numerical solution of eq.2 derives from a conservative 2nd order finite difference scheme employing a regular in space finite difference grid with constant step $\Delta x=\Delta z$, and constant time increment Δt, following Zahradnik (1989). The displacement at $t=(k+1)\Delta t$ is determined from the displacement at the two preceding levels $k\Delta t$ and $(k-1)\Delta t$:

$$\begin{aligned} u_{I,J}^{K+1} = 2u_{I,J}^{K} - u_{I,J}^{K-1} + \left(\frac{\Delta t}{\Delta x}\right)^2 [M_{I,J}^{H} u_{I,J+1}^{K} - \\ -(M_{I,J}^{H} + M_{I,J-1}^{H}) u_{I,J}^{K} + M_{I,J-1}^{H} u_{I,J-1}^{K} + M_{I,J}^{V} u_{I+1,J}^{K} - \\ -(M_{I,J}^{V} + M_{I+1,J}^{V}) u_{I,J}^{K} + M_{I-1,J}^{V} u_{I-1,J}^{K}] \end{aligned} \qquad (3)$$

Indices I and J are for the space discretization in the z and x coordinates. $M_{I,J}^{V}$ and $M_{I,J}^{H}$ represent the shear wave velocities squared. At the edges of the computation region the non-reflecting boundaries (absorbing boundary conditions), are imposed as described by Reynolds (1978) and the top of the grid is made a free surface.

In the FD run, we use a square grid of 2m and a time increment of 0.002s, which satisfies the stability conditions and assures negligible grid dispersion at frequencies lower than 10Hz.

In the first step of the calculations we compute an approximation to the impulse response of the 2-dimensional model of the region by exciting it with a simple delta-like impulse of short duration. As excitation signal we used a unipolar (one-sided) Ricker wavelet, whose zero frequency value is unity. Furthermore, absorption correction was implemented, based on a frequency independent Q model following Emmerich and Korn (1987).

Ten synthetic seismograms were obtained for ten sites along a W-E line crossing the city (Fig.4). There is a 78% increase in the value of peak acceleration towards the eastern end of the line, where the maximum peak acceleration was calculated (Fig.7).

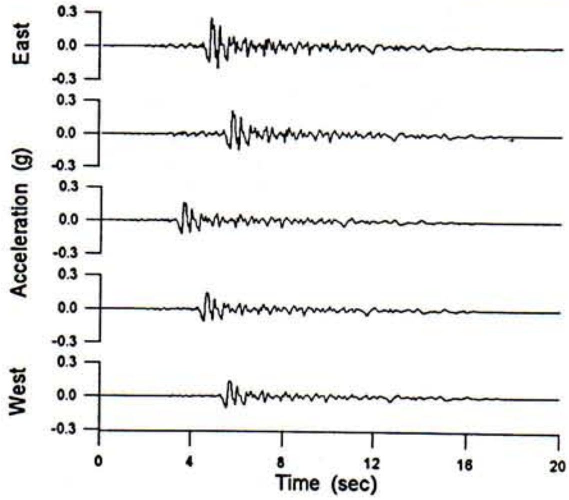

Fig.7 : The calculated synthetic seismograms along an W-E traverse crossing the city (only the seismograms corresponding to even number sites are shown).

Furthermore the response spectra of every synthetic seismogram was calculated. In Fig.8 we compare the PSV spectra of the western and the eastern site, respectively. There is an increase of PSV values close to a value of 0.1sec period which is comparable with the resonant period of buildings in the city.

All the above results are in good agreement with the macroseismic observations and explain the damage pattern in the city.

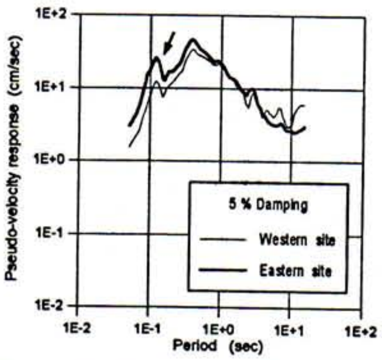

Fig.8 : Comparison of PSV spectra obtained for the western and eastern side of the city.

8 Conclusions

In the present study, we tried to explain the observed macroseismic data at the city of Vartholomio during the October 1988 earthquake. Using a subsurface structure derived from extensive geophysical and geotechnical investigations, a two-dimensional SH finite difference calculation explained the observed spatial damage variations of the macroseismic field. The analysis showed that the surface motions were affected by the combined effect of the presence of low velocity surface formations and the dipping topography of the seismic bedrock.

Acknowledgements

The authors wish to thank Hampson Russell software services for permitting access to GLI3D, Prof J.Zahradnik for his helpful comments during the processing stage, and Dr.N.S.Melis for his support during the preparation of this publication.

References

Emmerich H. and Korn M. (1987). Incorporation of attenuation into time-domain computations of seismic wave fields, *Geophysics*, 52, p.1252-1264.

Hampson D. and Russell B.H. (1984). First-break interpretation using generalised linear inversion, *Jr of the CSEG*, 20,1, p.40-54.

Idriss I.M., Sun J.I. (1992). SHAKE91 : A computer program for conducting equivalent linear seismic response analyses of horizontally layered soil deposits (Program modified based on the original SHAKE program), pp.13.

Lekkas E., Papanicolaou D. and Fountoulis I. (1992). Neotectonic map of Greece, sheets Pirgos and Tropea. Special report, University of Athens, 120pp.

Pitilakis K., Gariel J.C. and Bard P.Y. (1992). Investigation of the influence of seismic source, local geology and local soil conditions during Kalamata 1986 earthquake. Proceedings, First Greek Congress on Earthquake resistant Construction and Engineering Seismology, Athens, Vol1, p.80-91.

Reynolds A.C. (1978). Boundary conditions for the numerical solutions of wave propagation problems, *Geophysics*, 43, p.1099-1110.

Theodulidis N. and B.C. Papazachos (1992). Dependence of strong ground motion on magnitude-distance, site geology and macroseismic intensity for shallow, earthquakes in Greece: I. Peak horizontal acceleration, velocity and displacement. *Soil Dynamics and Earthquake Engineering*, 11, 387-402.

Tselentis G-A. (1993). Depth dependent seismic attenuation in Western Greece. *Tectonophysics*, 225, p.523-528.

Tselentis G-A. and Delis G. (1991). In situ rapid assessment of dynamic soil characteristics for microzonation investigations. Proceedings, Sixth International Congress, IAEG, Amsterdam, Proc. Vol2, p.893-899.

Tselentis G-A., Sokos E., Vasiliou J., Kalteziotis N. and Rubas D. (1994). Site conditions and site response at Dafnes, W.Greece during the Pirgos March 1993 earthquake sequence. Proceedings, second International Conference on Earthquake resistant Construction and Design, Berlin, Vol1, p.117-127.

Tselentis G-A., Vasiliou J and Kalteziotis N. (1992). Reassessment of the intensity of strong motions experienced by the suburb of Athens Halandri during the Corinth 1981 earthquake and comparison with macroseismic observations. Proceedings, International Symposium on the effects of Surface Geology on seismic motion, Odawara, Japan, Vol.2, p.143-149.

Zahradnik J. (1989). Synthesis of ground motion at building sites. Report of the building Research Institute, Prague, 80pp.